ACS Sustainable Chemistry & Engineering

Research Article

pubs.acs.org/journal/ascecg

Graphene Oxide as a Stabilizer for "Clean" Synthesis of High-Performance Pd-Based Nanotubes Electrocatalysts

Huan Zhang, Kai Cai, Pan Wang, Zhao Huang, Jiawei Liu, Long Wu, Mohamed F. Foda, and Heyou Han*

State Key Laboratory of Agricultural Microbiology, College of Science, Huazhong Agricultural University, Wuhan 430070, China

Supporting Information

ABSTRACT: By using graphene oxide (GO) as the stabilizing and dispersing agent in aqueous solution at room temperature, Pd-based (PdTe, PdPtTe, and PdAuTe) nanotubes (NTs)/GO nanocomposites were readily prepared. The obtained GO-supported one-dimensional (1D) Pd-based NTs have relatively uniform morphology and good dispersity. The catalytical properties of PdAuTe NTs/reduced GO (rGO) nanocomposites with different metal ratios were systematically investigated after electrochemical reduction process. $Pd_{47}Au_{33}Te_{20}$ nanotubes/rGO nanocomposites possess the optimal mass activity (5.31 mA ug^{-1}_{Pd}), which is 5.16-fold that of commercial Pd/C catalyst. The study provides a new strategy for clean synthesis of Pd-based NTs/GO nanocomposites, which are efficient catalysts for ethanol electrooxidation. It will probably inspire more appropriate utilization of graphene to design new hybrid materials with better properties applied in fuel cells or other related fields.

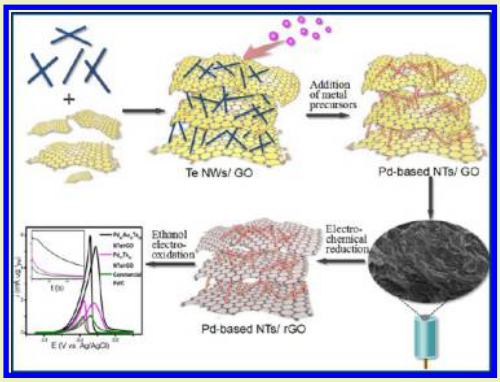

KEYWORDS: *Graphene oxide, Pd-based nanotubes, Stabilizing agent, Electrocatalyst, Ethanol oxidation*

INTRODUCTION

Development of electrochemical energy conversion devices is an effective route to meet the increasing demand for energy.[1−3] Direct ethanol alkaline fuel cells (DEAFCs) have received intense research attention in recent years due to the special advantages of ethanol, such as higher theoretical energy density (8 kW·h kg^{-1}) than methanol and formic acid and easier large-scale production directly from the fermentation of biomass.[4−6] In industrial and commercial applications of DEAFCs, the exploration of efficient and low-cost catalysts for ethanol electrooxidation should be given full consideration.[7]

It has been well-documented that the components, size, shape, and morphology as well as the supports are determinants of the catalytic activity of nanostructures.[8−11] Pt and Pt-based nanomaterials have been used as superior catalyst for DEAFCs due to the ultrahigh catalytic activity of Pt to break carbon bonds, but their inherent drawbacks hinder the sustainable development of DEAFCs.[7,12,13] Pd has been regarded as a competitive alternative of Pt when taking the reserve, cost, resistance to CO-poisoning, and reaction kinetics into account.[14] However, Pd has intrinsically low activity of cleaving carbon bond (C−C) and relatively weak stability when catalyzing ethanol electrooxidation.[15] To overcome this problem, other metals were incorporated into Pd materials to form Pd-based catalyst. So far, various Pd-based multi-component catalysts, including the low-Pt nanostructures such as PtPd- and PdPt-containing nanocrystals,[16−18] and non-Pt nanocatalysts such as PdAu, PdCu, PdFe, and PdRuTe nanostructures, have exhibited remarkably higher electro-catalytic activity and durability than their corresponding Pd counterparts.[12,19−21] Additionally, the one-dimensional (1D) nanostructures, especially hollow nanotubes, endow the catalysts with remarkable structure stability, catalytic property, and durability in contrast to zero-dimensional (0D) nano-particles.[6,22−26]

Moreover, to relieve the corrosion of common carbon supports and the resulting damage to the catalyst structure, promising support materials are an urgent need.[24,27,28] Graphene is single-layered and consists of carbon atoms with close-packed hexagonal lattices, possessing high electrical conductivity, large specific surface area, and mechanical flexibility.[29−32] It has been demonstrated that graphene or graphene oxide (GO) can be used as a superior support for electrocatalysis.[33,34] For example, graphene- or GO-supported Pd nanoparticles show high electrocatalytic ability for ethanol and formic acid oxidation.[35−38] Generally, there are two kinds of methods to prepare metal/graphene or metal/GO nano-composites: in situ growth and assembly after the preparation of metal nanoparticles. However, both methods have some defects. In the former, the morphology of nanoparticles can not be controlled well, and their distribution is usually not uniform.[36] In the latter, surfactant or stabilizing agent is often used in the preparation, which is generally difficult to be removed and will result in decrease of catalytic activity.[39]

Received: February 21, 2017
Revised: April 20, 2017
Published: May 7, 2017

DOI: 10.1021/acssuschemeng.7b00544
ACS Sustainable Chem. Eng. XXXX, XXX, XXX−XXX

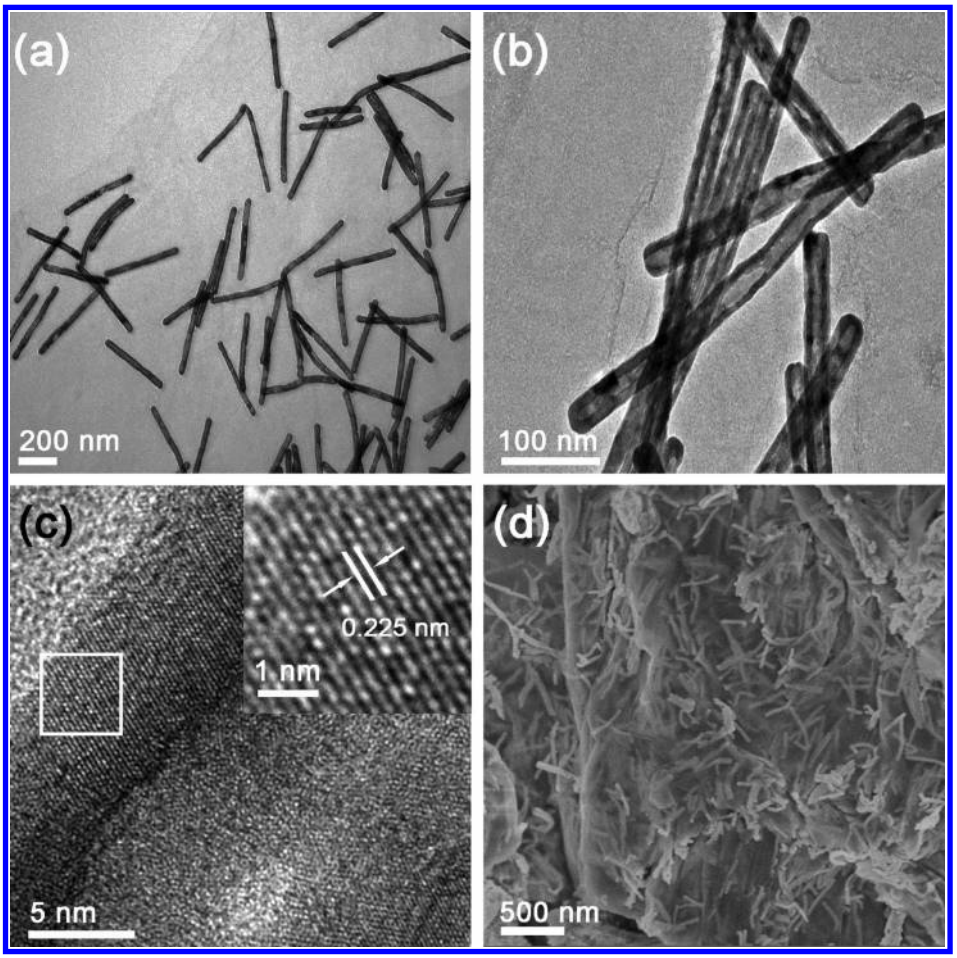

Figure 1. TEM (a–c) images with different resolutions and SEM (d) image of PdTe NTs/GO nanocomposites.

It is noteworthy that some recent works reported that GO could play a role of "surfactant" in the surfactant-free synthesis of nanostructured catalysts owing to its uniquely amphiphilic structure.[40,41] Therefore, it is possible to avoid both of the aforementioned defects to obtain metal/GO nanocomposites. To the best of our knowledge, there have been few reports about the surfactant-free synthesis of GO-supported nanotubes electrocatalysts up to now.

Herein, we report a facile and universal method for the clean synthesis of high-quality 1D Pd-based (PdTe, PdPtTe, and PdAuTe) nanotubes (NTs)/GO nanocomposites by using GO as a dispersing and stabilizing agent in template-directed synthesis. After electrochemical reduction process, the as-formed PdAuTe NTs/reduced GO (rGO) and PdTe NTs/rGO nanocomposites were used to electrocatalyze the ethanol oxidation reaction in alkaline. They exhibited higher electrocatalytic activity and durability than commercial Pd/C catalyst. In particular, the composition-optimized $Pd_{47}Au_{33}Te_{20}$ NTs/rGO nanocomposites possess the mass activity of 5.31 mA ug^{-1}_{Pd}, which is 5.16-fold that of commercial Pd/C catalyst. This study demonstrates that the Pd-based NTs/GO nanocomposites have the potential to be used as a highly efficient electrocatalyst for DEAFCs and that the facile method can probably inspire more utilization of graphene to design novel metal/GO nanocomposites.

EXPERIMENTAL SECTION

Reagents and Materials. Tellurium dioxide powder (TeO_2, 99.99%) was obtained from Aladdin Chemistry Co., Ltd. Hydrazine monohydrate ($N_2H_4{\cdot}H_2O$, 85%, AR), palladium(II) chloride ($PdCl_2$, AR), tetrachloroauric(III) acid hydrate ($HAuCl_4{\cdot}4H_2O$, AR), and potassium tetrachloroplatinate (II) (K_2PtCl_4, AR) were purchased from the Sinopharm Chemical Reagent Co., Ltd. Sodium dodecyl sulfate (SDS, 99%) was provided by Sigma-Aldrich. Commercial Pd/C (20 wt % on activated carbon) was obtained from Alfa Aesar (China) Chemicals Co., Ltd. GO was commercially available from Nanjing XFNANO Materials Tech Co., Ltd. All chemicals were used directly without any further purification.

Synthesis of Te Nanowires. Te nanowires (NWs) were prepared by following the method provided by Chang et al.[42] Simply, 10 mL of $N_2H_4{\cdot}H_2O$ was mixed with TeO_2 (0.032 g) powder under constant magnetic stirring at room temperature for about 30 min, with the color of the solution changing from colorless to blue. The mixture was 10-fold diluted with SDS (10 mM) for the closure of the growth of Te NWs and was then treated three times with a centrifugation/wash cycle. The residue was finally dispersed in 8 mL of ultrapure water.

Synthesis of Pd-Based NTs/GO Nanocomposites. The obtained Te NWs (0.4 mL) were mixed with GO (1 mL, 0.5 mg/mL). Next, $PdCl_2$ (2.5 μmol) and different amounts of $HAuCl_4$ (0.075 μmol, 0.15 μmol and 0.25 μmol) were added to the mixture together to prepare PdAuTe NTs/GO nanocomposites with Pd/Au/Te mass ratios of 62:17:21, 47:33:20, and 31:49:20, respectively. There was no $HAuCl_4$ addition when synthesizing PdTe NTs/GO nanocomposites. Stirring was continued for 15 min until the color changed from blue to dark yellow. Last, the nanocomposites were collected after centrifugation and washed by ultrapure water. When the $HAuCl_4$ precursor was replaced by K_2PtCl_4 (2.5 μmol), PdPtTe NTs/GO

DOI: 10.1021/acssuschemeng.7b00544
ACS Sustainable Chem. Eng. XXXX, XXX, XXX–XXX

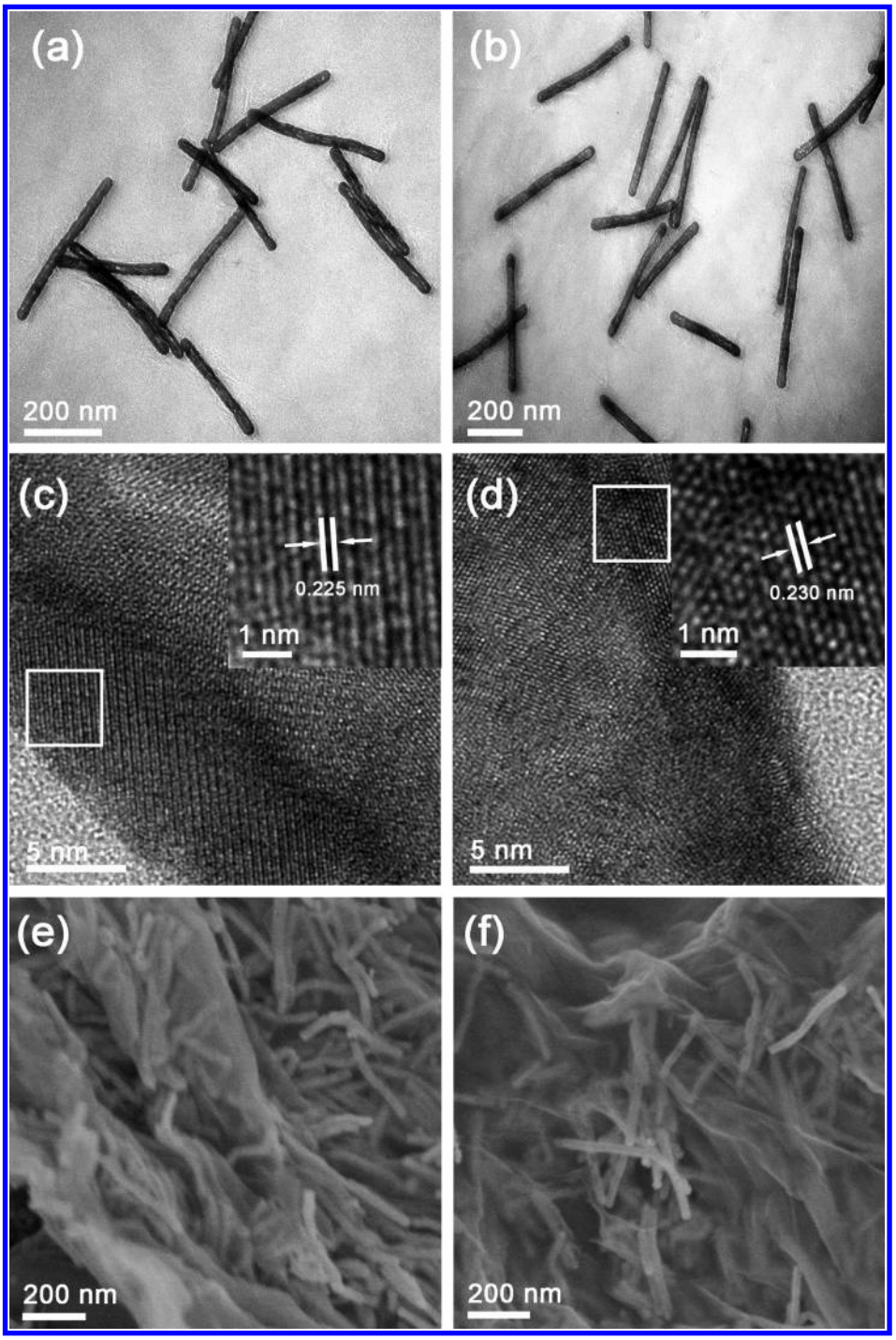

Figure 2. TEM (a, b), HRTEM (c, d), and SEM (e, f) images of PdPtTe NTs/GO and PdAuTe NTs/GO nanocomposites.

nanocomposites were synthesized. Eventually, the nanocomposites were electrochemically reduced for 200 s at the potential of −0.8 V in NaH_2PO_4 (0.1 M) solution after modifying them onto glassy carbon electrode (GCE).

Characterization. Transmission electron microscopy (TEM) images were recorded by a JEM-2100F high-resolution transmission electron microscope with an accelerating voltage of 200 kV. High-resolution transmission electron microscopy (HRTEM), cross-sectional line profiles, and energy-dispersive X-ray spectroscopy (EDS) analyses were measured in the high-angle annular dark field (HAADF) mode on a FEI TECNAIF-30 microscope operated at 300 kV. Scanning electron microscope (SEM) measurements were made on a field-emission scanning electron microscope (Bruker AXS Micro-analysis GmbH Berlin, Germany) at an accelerating voltage of 3 kV. X-ray diffraction (XRD) analysis was performed with a Bruker D8 Advance X-ray diffractometer using Cu Kα as radiation source. An IRIS Intrepid II XSP instrument (Thermo Fisher Scientific, USA) was used to perform the inductively coupled plasma atom emission spectroscopy (ICP-AES) measurements. Raman spectrum was obtained by an inVia Raman spectrometer (Renishaw, UK) equipped with a confocal microscope (Leica, German) using a 633 nm He−Ne laser excitation. The X-ray photoelectron spectroscopy (XPS) analysis was carried out on a Thermo Fisher ESCALAB 250Xi spectrophotometer with Al Kα radiator. Samples for TEM measurement were made by depositing a single drop of as-prepared nanocomposite solution dispersed in water on copper grids.

DOI: 10.1021/acssuschemeng.7b00544
ACS Sustainable Chem. Eng. XXXX, XXX, XXX−XXX

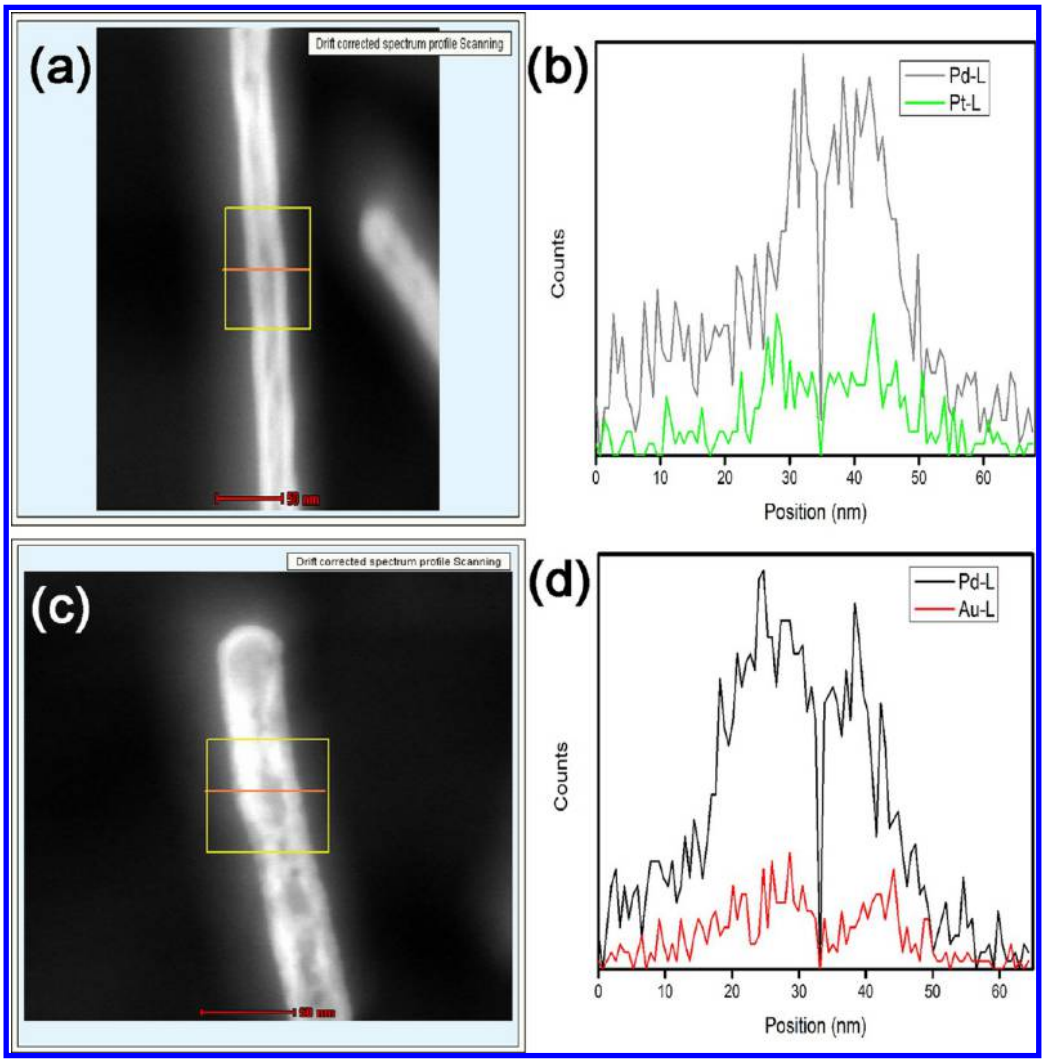

Figure 3. Cross-sectional compositional line profiles of PdPtTe NTs/GO and PdAuTe NTs/GO nanocomposites.

Electrochemical Measurements. Before the measurement, the GCE was polished by 1.0, 0.3, and 0.05 μm alumina powder and sonicated in 50% HNO_3 aqueous solution, then washed by ultrapure water. For the electrochemical experiments, an appropriate amount of the as-prepared nanocomposites or the commercial Pd/C suspension was dropped onto the GCE. After drying at room temperature, 0.28% Nafion (5 μL, dissolved in ethanol) was dropped to cover nanomaterials-modified GCE and air-dried before the electrochemical test. All the electrochemical measurements of ethanol electro-oxidation were carried out in a three-electrode cell on a CHI660D electrochemical workstation, Chenhua Instruments Corp (Shanghai, China). A platinum wire was used as auxiliary electrode, Ag/AgCl electrode was used as reference electrode, and a GCE (diameter = 3 mm, 0.07 cm^2) was used as the working electrode.

RESULTS AND DISCUSSION

The 1D Pd-based nanocomposites were prepared in an aqueous solution at room temperature by using Te NWs as both sacrificial templates and reducing agent in the presence of GO. Because there are a great deal of functional groups with negative charge in GO,[43] the Te NWs could disperse well in the solution. Through adding different metal precursors into the system, corresponding nanocomposites could be obtained because of the galvanic replace reaction between the precursors and the Te NWs.[44]

Initially, we used a Pd precursor in the synthesis to test the feasibility of the approach. The morphologies of the synthesized nanocomposites were characterized through transmission electron microscope (TEM) at first. Figure 1a shows that a large number of nanotubes with a uniform size (about 30 nm in diameter, 460 nm in length) are scattered among GO, and there is no particle with other morphologies, which preliminarily indicates that 1D Pd-based nanocomposites were successfully obtained. The TEM images with higher magnification in Figure 1b,c clearly reveal the hollow structure with the nanotube thickness being about 8 nm. Furthermore, the nanocomposites were analyzed by scanning electron microscope (SEM). A typical SEM image in Figure 1d confirms the obtainment of 1D NTs/GO nanocomposites. The EDS analysis (as shown in Figure S3) shows that there are Pd and Te in the sample in addition to C. The ICP-AES measurement further shows that the mass ratio of Pd to Te is 77:23. Because of a smaller amount of metal precursors, along with the coverage of GO, the diffusion of TeO_3^{2-} generated in the replacement reaction was slowed down, resulting in residual Te in the final product.[44,45] Previous studies have indicated that during the process of turning Te NWs into 1D nanotubes, the residual Te in the 1D nanostructure would be favorable to improving the utilization of the noble metals.[20,46] The HRTEM image reveals

DOI: 10.1021/acssuschemeng.7b00544
ACS Sustainable Chem. Eng. XXXX, XXX, XXX−XXX

that the observed lattice spacing is about 0.225 nm, which corresponds to the (111) interplanar distance of PdTe.[46] The X-ray diffraction (XRD) pattern of the product is depicted in Figure 4. The result displays that the as-formed PdTe NTs are face-centered cubic (*fcc*) crystals.[20,46] In addition, considering that the diffraction peak at 2θ = 40.05 is associated with the (111) facet of the *fcc* crystal, according to the Bragg equation ($d = \lambda/2 (\sin \theta)$), the d spacing of the lattice was calculated to be 0.225 nm, which is identical to that of the HRTEM. All of the above analyses demonstrate that the new method was successfully used to synthesize PdTe NTs/GO nanocomposites.

The valid method can be applied to prepare other Pd-based/GO nanocomposites, such as PdPtTe or PdAuTe NTs/GO nanocomposites, by only changing the metal precursors. Figure 2 shows the TEM and SEM images of the as-obtained PdPtTe NTs/GO and PdAuTe NTs/GO nanocomposites. It clearly shows that the NTs have a homogeneous size and that GO is well-mixed with them. The EDS analysis (Figures S4 and S5) shows that there are Pd, Pt, and Te in PdPtTe NTs/GO and Pd, Au, and Te in PdAuTe NTs/GO nanocomposites. Figure 2c,d shows the HRTEM images of single PdPtTe and PdAuTe NTs. The lattice spacing of 0.225 or 0.230 nm corresponds to the (111) interplanar distance of PdPtTe or PdAuTe, respectively. Moreover, the linear EDS scan across a single NT shown in Figure 3 reveals that Pd and Pt (or Au) are homogeneously distributed and that the 1D nanostructure is obviously hollow. The XRD pattern of the nanocomposites (Figure 4) shows that they are *fcc* crystals. Compared with the

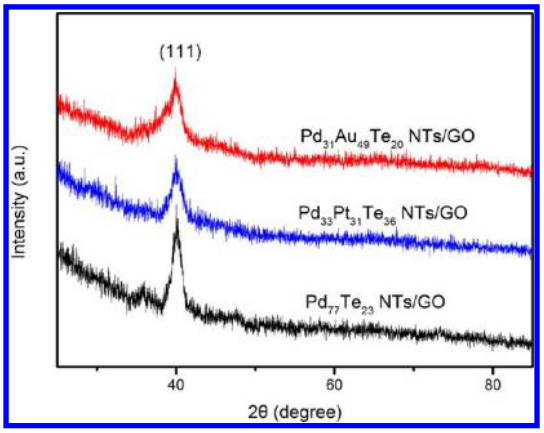

Figure 4. XRD patterns of $Pd_{77}Te_{23}$, $Pd_{33}Pt_{31}Te_{36}$, and $Pd_{31}Au_{49}Te_{20}$ nanotubes/GO nanocomposites.

diffraction peaks of PdTe NTs/GO nanocomposites, the peaks of PdPtTe NTs/GO and PdAuTe NTs/GO nanocomposites have lower diffraction angles, which is in conformity with the previous report.[46]

The PdAuTe NTs/GO electrocatalysts prepared without the use of stabilizing agent possess a superior support. More importantly, as a Pt-free catalyst, PdAu nanostructures have been demonstrated to have good electrocatalytic performance by many research groups. Feng et al. synthesized alloy PdAu nanoparticles with different atom ratios through coreducing the two metal precursors, and the catalysts showed enhanced electrocatalytic activity toward ethanol oxidation.[47] Hong et al. demonstrated that PdAu NW networks had superior catalytic performance in the process of ethanol electrooxidation.[19] Therefore, the new PdAuTe/GO nanostructures are expected to have good electrocatalytic properties.

In this study, PdAuTe NTs/GO nanocomposites with different Pd/Au mass ratios were prepared and used as electrocatalyst in ethanol oxidation. Figures 5 and S6 display the TEM and SEM images as well as the EDS results of the PdAuTe NTs/GO nanocomposites with different Pd/Au mass ratios (Figures S5, S7, and S8). The homogeneous nanotubes are obviously well-mixed with GO, and there are Pd, Au, and Te in all the three samples with different ratios. Moreover, the existence of GO was further proved by Raman spectrum successfully (Figure S9a).[39] ICP-AES analysis accurately showed that the mass ratios of the three nanocomposites were 62:17:21, 47:33:20, and 31:49:20, respectively.

The structure of the obtained nanocomposites was further studied by XPS. Figure 6 shows the XPS spectra of PdAuTe NTs/GO nanocomposites with different metal ratios and of $Pd_{77}Te_{23}$ NTs/GO nanocomposites. With the addition of Au, the Pd $3d_{5/2}$ and $3d_{3/2}$ peaks of PdAuTe NTs/GO nanocomposites with different metal ratios all shifted toward lower values when compared with that of $Pd_{77}Te_{23}$ NTs/GO nanocomposites, indicating the electronic structure modification of Pd caused by the incorporation of Au.[19,48,49] In addition, the peaks of $Pd_{62}Au_{17}Te_{21}$ NTs/GO nanocomposites had the slightest shift, while those of $Pd_{47}Au_{33}Te_{20}$ NTs/GO nanocomposites showed the most significant shift.

Subsequently, the catalytic activities of PdAuTe NTs/GO nanocomposites were investigated in alkaline solution. The measurement was conducted in 1.0 M KOH + 0.5 M ethanol solution using CV at the scan rate of 50 mV s^{-1} under room temperature. Before that, the GO in the nanocomposites had been electrochemically reduced. The Raman spectrum in Figure S9b demonstrates the reduction of GO in the nanocomposites.[39] Then, the catalysts were treated with CV scan in 0.5 M H_2SO_4 with scan rate of 100 mV s^{-1}, aiming to expose the active sites on metal surface and improve the stability.[46,50] 1D PdTe NTs/GO nanocomposites were used for comparison in the test and were processed by the same method. Before the tests for ethanol electrooxidation, the CV curves of the catalysts have been obtained in a N_2-saturated 1 M KOH (shown in Figure 7). Here, the apparent peaks appearing between −0.33 and −0.23 V in the negative scan were attributed to the reduction of the Pd oxides, which were formed on the catalysts surface during the positive scan.[47] Obviously, the peaks shifted to the positive position while the content of Au increased, implying that the surface activities of the catalysts have been influenced by Au.[47,51] Moreover, the electrochemically active surface area (ECSA) of the catalysts can be computed by measuring the Coulombic charge for the reduction of Pd oxides with proper conversion factor (see Supporting Information, eq 1).[47,51,52] The ECSA of $Pd_{47}Au_{33}Te_{20}$ NTs/rGO composites was 27.8 m^2 g^{-1}, which was larger than that of $Pd_{77}Te_{23}$ NTs/rGO composites (16.0 m^2 g^{-1}) and smaller than that of commercial Pd/C (48.3 m^2 g^{-1}).

Figure 8a,b shows the CV curves of the prepared PdAuTe or PdTe NTs/rGO nanocomposites and commercial Pd/C catalyst, in which the current density had been normalized on the basis of the mass of Pd. And Figure S10 displays corresponding CV curves and current−time curves by normalizing the current density with the total mass of metal. The mass activity for $Pd_{47}Au_{33}Te_{20}$ NTs/rGO nanocomposites is 5.31 mA μg^{-1}_{Pd}, which is nearly 5.16- and 2.90-fold that of commercial Pd/C (1.03 mA μg^{-1}_{Pd}) and $Pd_{77}Te_{23}$ NTs/rGO

DOI: 10.1021/acssuschemeng.7b00544
ACS Sustainable Chem. Eng. XXXX, XXX, XXX−XXX

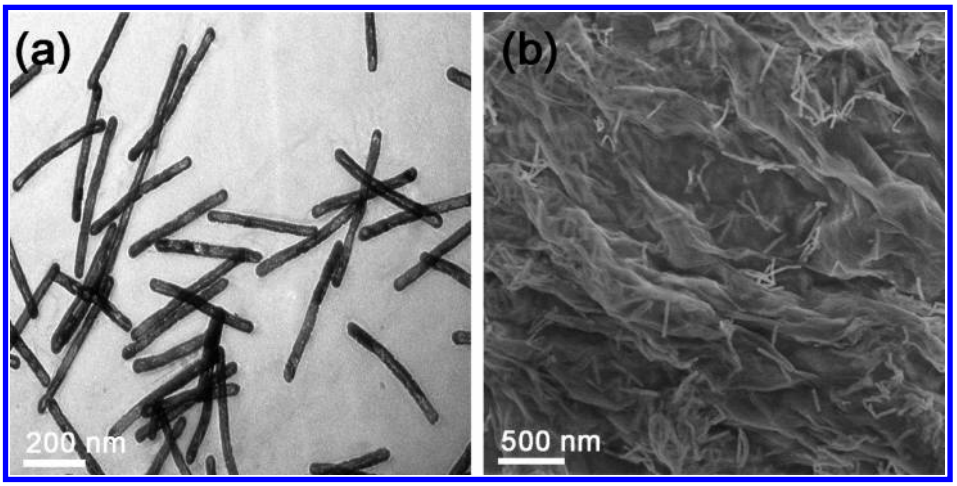

Figure 5. TEM (a) and corresponding SEM (b) images of $Pd_{47}Au_{33}Te_{20}$ NTs/GO nanocomposites.

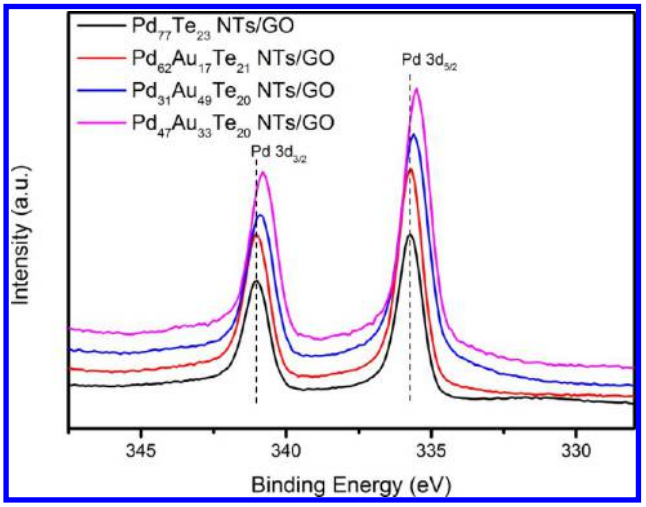

Figure 6. XPS spectra of PdAuTe NTs/GO nanocomposites with different metal ratios and $Pd_{77}Te_{23}$ NTs/GO nanocomposites.

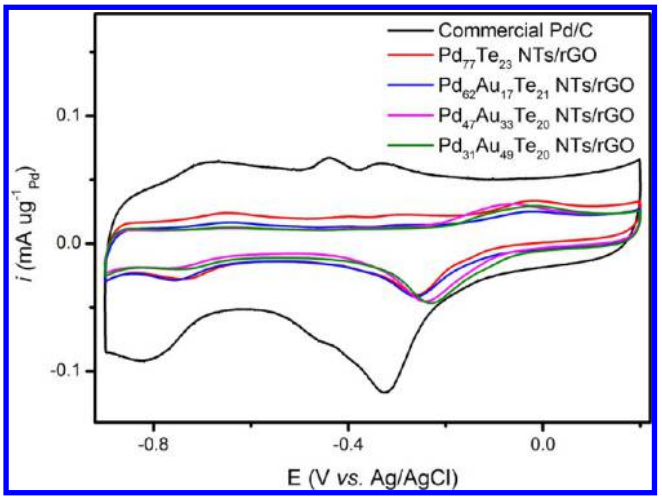

Figure 7. CV curves of $Pd_{77}Te_{23}$ NTs/rGO nanocomposites, PdAuTe NTs/rGO nanocomposites with different metal ratios, and commercial Pd/C catalyst, in a N_2-saturated 1 M KOH at a scan rate of 50 mV s^{-1}.

nanocomposites (1.83 mA μg^{-1}_{Pd}), respectively. The onset potential of $Pd_{47}Au_{33}Te_{20}$ NTs/rGO nanocomposites is much lower than that of commercial Pd/C, suggesting improved kinetics of electrooxidation reaction.[51] $Pd_{47}Au_{33}Te_{20}$ NTs/rGO nanocomposites also exhibited a higher mass activity (5.31 mA μg^{-1}_{Pd}) compared with $Pd_{62}Au_{17}Te_{21}$ NTs/rGO nanocomposites (2.94 mA μg^{-1}_{Pd}) and $Pd_{31}Au_{49}Te_{20}$ NTs/rGO nanocomposites (4.87 mA μg^{-1}_{Pd}). Table S1 shows the related data and results of ethanol electrooxidation experiment in alkaline.

In addition, the stability of catalysts was examined by long-term current−time curve measurement at −0.3 V for 1800 s in 0.5 M ethanol + 1.0 M KOH solution, and the results are depicted in Figure 8c. At the beginning, there was an obvious current decay for all the catalysts. This phenomenon may be caused by the incomplete oxidation of ethanol, in which some poisonous carbonaceous intermediates are generated and then adsorbed on the surface of catalysts, covering up the surface active sites.[39] After that, the as-prepared PdAuTe NTs/rGO catalysts exhibited effective resistance to current decay compared with PdTe NTs/rGO nanocomposites and commercial Pd/C, implying that the incorporation of Au could apparently improve the stability of Pd-based electrocatalysts. Moreover, the comparisons of the catalytic activities before and after the stability tests are displayed in Figure S11. The $Pd_{47}Au_{33}Te_{20}$ NTs/rGO nanocomposites retained a similar catalytic activity after the test, and all of the as-prepared nanocomposites showed slower activity decline compared with that of commercial Pd/C, showing the enhanced stability of the as-prepared electrocatalysts.

The notable enhancement of the catalytic activity and durability of the Pd-based NTs/rGO nanocomposites can be ascribed to the following reasons: (1) GO, which acts as stabilizing agent in the surfactant-free synthesis of nanocomposites, can effectively prevent the active sites from being capped by other surfactants and stabilizers.[36,39,53] Additionally, when compared with those general carbon supports, such as activated carbon and carbon black, GO possesses the merits of great dispersity and less possibility of severe corrosion and oxidation.[30,40] The electrochemical reduction could increase its conductivity as well,[43,54] and the synergistic effect of rGO with NTs can contribute to higher catalytic properties.[55,56] (2) The special 1D NTs/rGO nanocomposites structure could effectively avoid the common disadvantages of the corresponding carbon-supported 0D nanomaterials, i.e., degradation of the catalyst caused by the intrinsic morphology feature or the corrosion of the support.[6,22,23] It seems that the 1D nanostructure might act as a support in turn to prevent the

DOI: 10.1021/acssuschemeng.7b00544
ACS Sustainable Chem. Eng. XXXX, XXX, XXX−XXX

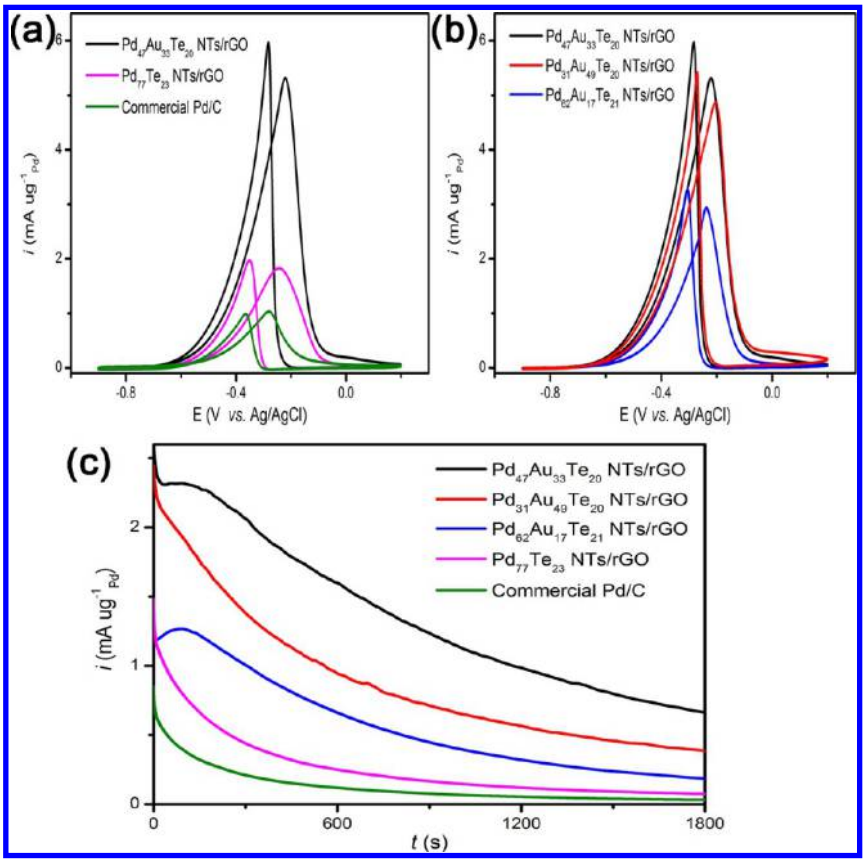

Figure 8. CV curves (a and b) and current−time curves (c) of $Pd_{77}Te_{23}$, PdAuTe NTs/GO nanocomposites and commercial Pd/C catalyst in 1.0 M KOH containing 0.5 M ethanol. The scan rate of CV is 50 mV s^{-1}.

stack of rGO,[57] which may be conducive for the exposure of active sites and be prone to provide open space for electrolyte diffusion around the metal catalysts during the electrocatalysis process.[58] (3) The appropriate incorporation of Au has a positive effect on the catalytic activity and durability of Pd-based nanostructures. The XPS results showed that the binding energies of Pd in PdAuTe NTs/GO nanocomposites shifted to lower values with the addition of Au in general. Particularly, the shift in $Pd_{47}Au_{33}Te_{20}$ NTs/rGO nanocomposites exhibiting the best catalytic properties in the electrochemical experiments was the largest. Previous studies proved that through modifying the electron structure and the distribution of Pd on the catalyst surface Au could influence the bond between Pd and the reactants or products and facilitate the formation of active sites of Pd catalysts.[51] However, if the amount of Au is super-abundant, then the catalytic activity would decline as excess Au with less catalytic activity would replace active Pd on the surface.[59,60]

CONCLUSIONS

We have developed a universal and "clean" method to synthesize 1D Pd-based (PdTe, PdPtTe, and PdAuTe) NTs/GO nanocomposites in aqueous solution at room temperature. GO plays a crucial role as the stabilizing and dispersing agent of the Te NWs template in the synthesis and serves as the support of the resulting hybrid catalyst. After electrochemical reduction process, the catalytic properties of PdTe and PdAuTe NTs/rGO nanocomposites with different mass ratios were investigated. They exhibited enhanced electrocatalytic ability for ethanol oxidation compared with commercial Pd/C catalysts in alkaline. Specially, the $Pd_{47}Au_{33}Te_{20}$ NTs/rGO nanocomposites exhibited the highest mass activity of 5.31 mA μg^{-1}_{Pd}, which is 5.16-fold that of commercial Pd/C catalyst. This study proposes a surfactant-free strategy to synthesize GO-based hybrid materials with controlled morphology, and it will probably inspire further utilization of graphene to design various efficient nanocatalysts for fuel cells or other electrochemical energy conversion devices.

ASSOCIATED CONTENT

Supporting Information

The Supporting Information is available free of charge on the ACS Publications website at DOI: 10.1021/acssuschemeng.7b00544.

Digital photo of the materials in different stages of reaction, TEM and corresponding SEM images, EDS spectra, Raman spectra with different mass ratios before and after the electrochemical reduction treatment, experimental data and results related to the ethanol electrooxidation, and CV curves and current−time curves (PDF)

AUTHOR INFORMATION

Corresponding Author

*E-mail: hyhan@mail.hzau.edu.cn.

ORCID

Heyou Han: 0000-0001-9406-0722

Author Contributions

H.Z. and K.C. contributed equally to the creation of this work.

DOI: 10.1021/acssuschemeng.7b00544
ACS Sustainable Chem. Eng. XXXX, XXX, XXX−XXX

Notes

The authors declare no competing financial interest.

■ ACKNOWLEDGMENTS

We acknowledge the financial supports from the National Natural Science Foundation of China (21375043 and 21175051). We thank Prof. Zuoxiong Liu for modifying the language.

■ REFERENCES

(1) Chen, A. C.; Holt-Hindle, P. Platinum-Based Nanostructured Materials: Synthesis, Properties, and Applications. *Chem. Rev.* **2010**, *110*, 3767−3804.
(2) Antolini, E. Palladium in Fuel Cell Catalysis. *Energy Environ. Sci.* **2009**, *2*, 915−931.
(3) Brouzgou, A.; Song, S. Q.; Tsiakaras, P. Low and non-Platinum Electrocatalysts for PEMFCs: Current Status, Challenges and Prospects. *Appl. Catal., B* **2012**, *127*, 371−388.
(4) Yang, Y.-Y.; Ren, J.; Li, Q.-X.; Zhou, Z.-Y.; Sun, S.-G.; Cai, W.-B. Electrocatalysis of Ethanol on a Pd Electrode in Alkaline Media: An in *Situ* Attenuated Total Reflection Surface-Enhanced Infrared Absorption Spectroscopy Study. *ACS Catal.* **2014**, *4*, 798−803.
(5) Yin, Z.; Lin, L. L.; Ma, D. Construction of Pd-Based Nanocatalysts for Fuel Cells: Opportunities and Challenges. *Catal. Sci. Technol.* **2014**, *4*, 4116−4128.
(6) Guo, S.; Dong, S.; Wang, E. Pt/Pd Bimetallic Nanotubes with Petal-like Surfaces for Enhanced Catalytic Activity and Stability towards Ethanol Electrooxidation. *Energy Environ. Sci.* **2010**, *3*, 1307−1310.
(7) Wu, F.; Zhang, D.; Peng, M.; Yu, Z.; Wang, X.; Guo, G.; Sun, Y. Microfluidic Synthesis Enables Dense and Uniform Loading of Surfactant-Free PtSn Nanocrystals on Carbon Supports for Enhanced Ethanol Oxidation. *Angew. Chem., Int. Ed.* **2016**, *55*, 4952−4956.
(8) Liu, S.; Tian, N.; Xie, A. Y.; Du, J. H.; Xiao, J.; Liu, L.; Sun, H. Y.; Cheng, Z. Y.; Zhou, Z. Y.; Sun, S. G. Electrochemically Seed-Mediated Synthesis of Sub-10 nm Tetrahexahedral Pt Nanocrystals Supported on Graphene with Improved Catalytic Performance. *J. Am. Chem. Soc.* **2016**, *138*, 5753−5756.
(9) You, H.; Yang, S.; Ding, B.; Yang, H. Synthesis of Colloidal Metal and Metal Alloy Nanoparticles for Electrochemical Energy Applications. *Chem. Soc. Rev.* **2013**, *42*, 2880−2904.
(10) Liu, B.; Yao, H.; Song, W.; Jin, L.; Mosa, I. M.; Rusling, J. F.; Suib, S. L.; He, J. Ligand-Free Noble Metal Nanocluster Catalysts on Carbon Supports via "Soft" Nitriding. *J. Am. Chem. Soc.* **2016**, *138*, 4718−4721.
(11) Gao, Y.; Chen, X.; Zhang, J.; Asakura, H.; Tanaka, T.; Teramura, K.; Ma, D.; Yan, N. Popping of Graphite Oxide: Application in Preparing Metal Nanoparticle Catalysts. *Adv. Mater.* **2015**, *27*, 4688−4694.
(12) Wang, Y.; He, Q.; Guo, J.; Wang, J.; Luo, Z.; Shen, T. D.; Ding, K.; Khasanov, A.; Wei, S.; Guo, Z. Ultrafine FePd Nanoalloys Decorated Multiwalled Cabon Nanotubes toward Enhanced Ethanol Oxidation Reaction. *ACS Appl. Mater. Interfaces* **2015**, *7*, 23920−23931.
(13) Zhang, G.; Yang, Z.; Zhang, W.; Hu, H.; Wang, C.; Huang, C.; Wang, Y. Tailoring the Morphology of Pt_3Cu_1 Nanocrystals Supported on Graphene Nanoplates for Ethanol Oxidation. *Nanoscale* **2016**, *8*, 3075−3084.
(14) Chen, A.; Ostrom, C. Palladium-Based Nanomaterials: Synthesis and Electrochemical Applications. *Chem. Rev.* **2015**, *115*, 11999−12044.
(15) Bianchini, C.; Shen, P. K. Palladium-Based Electrocatalysts for Alcohol Oxidation in Half Cells and in Direct Alcohol Fuel Cells. *Chem. Rev.* **2009**, *109*, 4183−4206.
(16) Lv, J.; Wisitruangsakul, N.; Feng, J.; Luo, J.; Fang, K.; Wang, A. Biomolecule-Assisted Synthesis of Porous PtPd Alloyed Nanoflowers Supported on Reduced Graphene Oxide with Highly Electrocatalytic Performance for Ethanol Oxidation and Oxygen Reduction. *Electrochim. Acta* **2015**, *160*, 100−107.
(17) Liu, Q.; Xu, Y.; Wang, A.; Feng, J. A Single-Step Route for Large-Scale Synthesis of Coreeshell Palladium@Platinum Dendritic Nanocrystals/Reduced Graphene Oxide with Enhanced Electrocatalytic Properties. *J. Power Sources* **2016**, *302*, 394−401.
(18) Hong, J. W.; Kim, Y.; Wi, D. H.; Lee, S.; Lee, S.-U.; Lee, Y. W.; Choi, S.-I.; Han, S. W. Ultrathin Free-Standing Ternary-Alloy Nanosheets. *Angew. Chem., Int. Ed.* **2016**, *55*, 2753−2758.
(19) Hong, W.; Wang, J.; Wang, E. Facile Synthesis of Highly Active PdAu Nanowire Networks as Self-supported Electrocatalyst for Ethanol Electrooxidation. *ACS Appl. Mater. Interfaces* **2014**, *6*, 9481−9487.
(20) Liu, J.; Huang, Z.; Cai, K.; Zhang, H.; Lu, Z.; Li, T.; Zuo, Y.; Han, H. Clean Synthesis of an Economical 3D Nanochain Network of PdCu Alloy with Enhanced Electrocatalytic Performance towards Ethanol Oxidation. *Chem. - Eur. J.* **2015**, *21*, 17779−17785.
(21) Hong, W.; Wang, J.; Wang, E. RuTe/M (M = Pt, Pd) Nanoparticle Nanotubes with Enhanced Electrocatalytic Activity. *J. Mater. Chem. A* **2015**, *3*, 13642−13647.
(22) Chen, Z.; Waje, M.; Li, W.; Yan, Y. Supportless Pt and PtPd Nanotubes as Electrocatalysts for Oxygen-Reduction Reactions. *Angew. Chem., Int. Ed.* **2007**, *46*, 4060−4063.
(23) Alia, S. M.; Zhang, G.; Kisailus, D.; Li, D.; Gu, S.; Jensen, K.; Yan, Y. Porous Platinum Nanotubes for Oxygen Reduction and Methanol Oxidation Reactions. *Adv. Funct. Mater.* **2010**, *20*, 3742−3746.
(24) Alia, S. M.; Jensen, K. O.; Pivovar, B. S.; Yan, Y. Platinum-Coated Palladium Nanotubes as Oxygen Reduction Reaction Electrocatalysts. *ACS Catal.* **2012**, *2*, 858−863.
(25) Xia, B. Y.; Ng, W. T.; Wu, H. B.; Wang, X.; Lou, X. W. Self-Supported Interconnected Pt Nanoassemblies as Highly Stable Electrocatalysts for Low-Temperature Fuel Cells. *Angew. Chem., Int. Ed.* **2012**, *51*, 7213−7216.
(26) Zheng, J.; Cullen, D. A.; Forest, R. V.; Wittkopf, J. A.; Zhuang, Z.; Sheng, W.; Chen, J. G.; Yan, Y. Platinum-Ruthenium Nanotubes and Platinum-Ruthenium Coated Copper Nanowires As Efficient Catalysts for Electro-Oxidation of Methanol. *ACS Catal.* **2015**, *5*, 1468−1474.
(27) Zhang, S.; Shao, Y.; Yin, G.; Lin, Y. Recent Progress in Nanostructured Electrocatalysts for PEM Fuel Cells. *J. Mater. Chem. A* **2013**, *1*, 4631−4641.
(28) Wu, X.; Shi, Z.; Fu, S.; Chen, J.; Berry, R. M.; Tam, K. C. Strategy for Synthesizing Porous Cellulose Nanocrystal Supported Metal Nanocatalysts. *ACS Sustainable Chem. Eng.* **2016**, *4*, 5929−5935.
(29) Huang, X.; Qi, X.; Boey, F.; Zhang, H. Graphene-Based Composites. *Chem. Soc. Rev.* **2012**, *41*, 666−686.
(30) Huang, Z.; Zhou, H.; Li, C.; Zeng, F.; Fu, C.; Kuang, Y. Preparation of Well-Dispersed PdAu Bimetallic Nanoparticles on Reduced Graphene Oxide Sheets with Excellent Electrochemical Activity for Ethanoloxidation in Alkaline Media. *J. Mater. Chem.* **2012**, *22*, 1781−1785.
(31) Cho, K. Y.; Seo, H. Y.; Yeom, Y. S.; Kumar, P.; Lee, A. S.; Baek, K. Y.; Yoon, H. G. Stable 2D-Structured Supports Incorporating Ionic Block Copolymer-Wrapped Carbon Nanotubes with Graphene Oxide toward Compact Decoration of Metal Nanoparticles and High-Performance Nanocatalysis. *Carbon* **2016**, *105*, 340−352.
(32) Kumar, R.; Oh, J. H.; Kim, H. J.; Jung, J. H.; Jung, C. H.; Hong, W. G.; Kim, H. J.; Park, J. Y.; Oh, Il-K. Nanohole-Structured and Palladium-Embedded 3D Porous Graphene for Ultrahigh Hydrogen Storage and CO Oxidation Multifunctionalities. *ACS Nano* **2015**, *9*, 7343−7351.
(33) Zhu, C.; Dong, S. Synthesis of Graphene-Supported Noble Metal Hybrid Nanostructures and Their Applications as Advanced Electrocatalysts for Fuel Cells. *Nanoscale* **2013**, *5*, 10765−10775.
(34) Zhu, C.; Dong, S. Recent Progress in Graphene-Based Nanomaterials as Advanced Electrocatalysts towards Oxygen Reduction Reaction. *Nanoscale* **2013**, *5*, 1753−1767.

DOI: 10.1021/acssuschemeng.7b00544
ACS Sustainable Chem. Eng. XXXX, XXX, XXX−XXX

(35) Jin, T.; Guo, S.; Zuo, J.-l.; Sun, S. Synthesis and Assembly of Pd Nanoparticles on Graphene for Enhanced Electrooxidation of Formic Acid. *Nanoscale* **2013**, *5*, 160−163.
(36) Chen, X.; Wu, G.; Chen, J.; Chen, X.; Xie, Z.; Wang, X. Synthesis of "Clean" and Well-Dispersive Pd Nanoparticles with Excellent Electrocatalytic Property on Graphene Oxide. *J. Am. Chem. Soc.* **2011**, *133*, 3693−3695.
(37) Kumar, R.; Savu, R.; Singh, R. K.; Joanni, E.; Singh, D. P.; Tiwari, V. S.; Vaz, A. R.; da Silva, E. T.S.G.; Maluta, J. R.; Kubota, L. T.; Moshkalev, S. A. Controlled Density of Defects Assisted Perforated Structure in Reduced Graphene Oxide Nanosheets-Palladium Hybrids for Enhanced Ethanol Electro-Oxidation. *Carbon* **2017**, *117*, 137−146.
(38) Kumar, R.; Singh, R. K.; Singh, D. P.; Vaz, A. R.; Yadav, R. R.; Rout, C. S.; Moshkalev, S. A. Synthesis of Self-Assembled and Hierarchical Palladium-CNTs-Reduced Graphene Oxide Composites for Enhanced Field Emission Properties. *Mater. Des.* **2017**, *122*, 110−117.
(39) Ren, F.; Wang, H.; Zhai, C.; Zhu, M.; Yue, R.; Du, Y.; Yang, P.; Xu, J.; Lu, W. Clean Method for the Synthesis of Reduced Graphene Oxide-Supported PtPd Alloys with High Electrocatalytic Activity for Ethanol Oxidation in Alkaline Medium. *ACS Appl. Mater. Interfaces* **2014**, *6*, 3607−3614.
(40) Kim, J.; Cote, L. J.; Huang, J. X. Two Dimensional Soft Material: New Faces of Graphene Oxide. *Acc. Chem. Res.* **2012**, *45*, 1356−1364.
(41) Zhang, Y.; Zhang, N.; Tang, Z.-R.; Xu, Y.-J. Graphene Oxide as a Surfactant and Support for In-Situ Synthesis of Au-Pd Nanoalloys with Improved Visible Light Photocatalytic Activity. *J. Phys. Chem. C* **2014**, *118*, 5299−5308.
(42) Lin, Z.-H.; Yang, Z.; Chang, H.-T. Preparation of Fluorescent Tellurium Nanowires at Room Temperature. *Cryst. Growth Des.* **2008**, *8*, 351−357.
(43) Chen, D.; Feng, H.; Li, J. Graphene Oxide: Preparation, Functionalization, and Electrochemical Applications. *Chem. Rev.* **2012**, *112*, 6027−6053.
(44) Liang, H.-W.; Liu, S.; Gong, J.-Y.; Wang, S.-B.; Wang, L.; Yu, S.-H. Ultrathin Te Nanowires: An Excellent Platform for Controlled Synthesis of Ultrathin Platinum and Palladium Nanowires/Nanotubes with Very High Aspect Ratio. *Adv. Mater.* **2009**, *21*, 1850−1854.
(45) Huang, Z.; Zhou, H.; Sun, F.; Fu, C.; Zeng, F.; Li, T.; Kuang, Y. Facile Self-Assembly Synthesis of PdPt Bimetallic Nanotubes with Good Performance for Ethanol Oxidation in an Alkaline Medium. *Chem. - Eur. J.* **2013**, *19*, 13720−13725.
(46) Li, H. H.; Zhao, S.; Gong, M.; Cui, C. H.; He, D.; Liang, H. W.; Wu, L.; Yu, S. H. Ultrathin PtPdTe Nanowires as Superior Catalysts for Methanol Electrooxidation. *Angew. Chem., Int. Ed.* **2013**, *52*, 7472−7476.
(47) Feng, Y.-Y.; Liu, Z.-H.; Xu, Y.; Wang, P.; Wang, W.-H.; Kong, D.-S. Highly Active PdAu Alloy Catalysts for Ethanol Electro-Oxidation. *J. Power Sources* **2013**, *232*, 99−105.
(48) Zhu, C.; Guo, S.; Dong, S. PdM (M = Pt, Au) Bimetallic Alloy Nanowires with Enhanced Electrocatalytic Activity for Electro-oxidation of Small Molecules. *Adv. Mater.* **2012**, *24*, 2326−2331.
(49) Hong, W.; Shang, C.; Wang, J.; Wang, E. Bimetallic PdPt Nanowire Networks with Enhanced Electrocatalytic Activity for Ethylene Glycol and Glycerol Oxidation. *Energy Environ. Sci.* **2015**, *8*, 2910−2915.
(50) Jiao, L.; Li, F.; Li, X.; Ren, R.; Li, J.; Zhou, X.; Jin, J.; Li, R. Ultrathin PdTe nanowires Anchoring Reduced Graphene Oxide Cathodes for Efficient Hydrogen Evolution Reaction. *Nanoscale* **2015**, *7*, 18441−18445.
(51) Chen, L. Y.; Chen, N.; Hou, Y.; Wang, Z. C.; Lv, S. H.; Fujita, T.; Jiang, J. H.; Hirata, A.; Chen, M. W. Geometrically Controlled Nanoporous PdAu Bimetallic Catalysts with Tunable Pd/Au Ratio for Direct Ethanol Fuel Cells. *ACS Catal.* **2013**, *3*, 1220−1230.
(52) Pan, W.; Zhang, X.; Ma, H. Y.; Zhang, J. T. Electrochemical Synthesis, Voltammetric Behavior, and Electrocatalytic Activity of Pd Nanoparticles. *J. Phys. Chem. C* **2008**, *112*, 2456−2461.
(53) Chen, X.; Cai, Z.; Chen, X.; Oyama, M. Green Synthesis of Graphene-PtPd Alloy Nanoparticles with High Electrocatalytic Performance for Ethanol Oxidation. *J. Mater. Chem. A* **2014**, *2*, 315−320.
(54) Kim, F.; Cote, L. J.; Huang, J. Graphene Oxide: Surface Activity and Two-Dimensional Assembly. *Adv. Mater.* **2010**, *22*, 1954−1958.
(55) Kumar, R.; Singh, R. K.; Singh, D. P.; Savu, R.; Moshkalev, S. A. Microwave Heating Time Dependent Synthesis of Various Dimensional Graphene Oxide Supported Hierarchical ZnO Nanostructures and Its Photoluminescence Studies. *Mater. Des.* **2016**, *111*, 291−300.
(56) Singh, R. K.; Kumar, R.; Singh, D. P. Graphene Oxide: Strategies for Synthesis, Reduction and Frontier Applications. *RSC Adv.* **2016**, *6*, 64993−65011.
(57) Yang, J.; Yu, C.; Fan, X.; Zhao, C.; Qiu, J. Ultrafast Self-Assembly of Graphene Oxide-Induced Monolithic NiCo-Carbonate Hydroxide Nanowire Architectures with a Superior Volumetric Capacitance for Supercapacitors. *Adv. Funct. Mater.* **2015**, *25*, 2109−2116.
(58) Kumar, R.; Singh, R. K.; Vaz, A. R.; Savu, R.; Moshkalev, S. A. Self-Assembled and One-Step Synthesis of Interconnected 3D Network of Fe_3O_4/Reduced Graphene Oxide Nanosheets Hybrid for High-Performance Supercapacitor Electrode. *ACS Appl. Mater. Interfaces* **2017**, *9*, 8880−8890.
(59) Gao, F.; Goodman, D. W. Pd-Au Bimetallic Catalysts: Understanding Alloy Effects from Planar Models and (Supported) Nanoparticles. *Chem. Soc. Rev.* **2012**, *41*, 8009−8020.
(60) Lai, S. C. S.; Kleijn, S. E. F.; Öztürk, F. T. Z.; van Rees Vellinga, V. C.; Koning, J.; Rodriguez, P.; Koper, M. T. M. Effects of Electrolyte pH and Composition on the Ethanol Electro-Oxidation Reaction. *Catal. Today* **2010**, *154*, 92−104.

DOI: 10.1021/acssuschemeng.7b00544
ACS Sustainable Chem. Eng. XXXX, XXX, XXX−XXX